A Hybrid Mathematical Programming Model for Densities of Alkanol + Alkanediol Mixtures Using Bacterial Foraging Optimization Algorithm

Noorzad, Fazel; Pirdashti, Mohsen*+

Chemical Engineering Department, Faculty of Engineering, Shomal University, PO Box 731 Amol, I.R. IRAN

Dragoi, Elena Niculina•

Faculty of Chemical Engineering and Environmental Protection "Cristofor Simionescu", "Gh. Asachi" Technical University, Bld. Mangeron 73, 700050, Iasi, ROMANIA

Babaei Nobijari, Yousef

Chemical Engineering Department, Faculty of Engineering, Shomal University, PO Box 731 Amol, I.R. IRAN

ABSTRACT: *In this work, the densities of pure and binary mixtures of 1-pentanol or 1-decanol with 1,2-ethanediol or 1,2-propanediol or 1,3-butanediol or 2,3-butanediol were measured at atmospheric pressure and temperatures between 288.15K and 313.15K. For the considered system, two types of models were applied: black box and phenomenological. The black box model is represented by Artificial Neural Networks (ANNs) optimized with an improved version of Bacterial Foraging Optimization (iBFO). The phenomenological models are represented by Spencer-Danner and Li equations. In addition, in order to better fit the Spencer-Danner and Li equations to the obtained experimental data, the free parameters of these models were included in an iBFO algorithm. The average absolute error of the best ANN obtained was 2.82%, while the new forms of the Spencer-Danner and Li equations had an improvement from 26.31% and 26.51% respectively to 3.51% and 4.01% respectively. These results indicate the flexibility and efficiency of iBFO, which can provide good solutions for various cases.*

KEYWORDS: *Density; Spencer–Danner equation; Alkanol; Alkanediol; Improved bacterial foraging optimization.*

INTRODUCTION

Density is an important physical property, its measurement being essential in the design of new processes at industrial scale. In addition, the experimental data of density of binary mixtures are quintessential for understanding the liquid theory, determination of fundamental properties (such as the coefficient of isothermal

compressibility and the coefficient of isobaric thermal expansion), and development and test of equations of state (especially in mass and moment balances) [1-3]. Because hydrogen bonds play a vital role in most chemical, physical, and biological processes, hydrogen-bonded systems are very common. It is well known that alcohols are highly associated with hydrogen bonds; thus, their structure and properties are determined mainly by quasi-chemical bonds between the molecules, which result in the formation of multimers of different sizsizesd structure. Especially interesting are diols, both from the practical and theoretical point of view [4]. Alkanols and alkanediols are important compounds that used in various applications. Their physiochemical properties are influenced by the hydroxyl group and therefore, they can be used for evaluating the hydrophobic interactions determined through theoretical models [5, 6]. Consequently, this work focuses on alkanols and alkanediols and their mixtures.

In this context, reliable values for the properties of these material are necessary, especially when designing and implementing small or large-scale industrial processes. Many works focused on this aspect, entire datasets being collected and correlated. However, as the technology advances, the gap between demand and availability of data seems to remain constant. Therefore, in a stride to reduce the necessity of experimental measured values, strategies and method for predicting material properties were developed [7]. A number of investigators have developed equations for predicting the density of mixtures [8-12]. Also, generalized methods for predicting the saturated liquid density of pure compounds determined on a large set of critically evaluated experimental density data were proposed. Compared to other equations, the Spencer-Danner version of the Rackett equation with one adjustable constant, Z_{RA}, determined from the experimental data and Li equation are shown to be slightly more accurate. These equations also compare favorably to the other equations in terms of availability of input parameters, range of application, and ease of use [7, 9].

The majority of works so far focus on the system's phenomenology, analytical correlation and/or statistical analysis. In the latest years, artificial neural networks (ANN) provide a range of powerful new techniques for solving problems in sensor data analysis, fault detection, process identification, and control and have been used in a diverse range of chemical engineering applications [13].

Artificial intelligence-based techniques were also used for determining/predicting properties of mixtures such as density of two-phase mixtures [14,15] of binary mixture of ionic liquids+ water [16, 17], flow regime in gas-liquid two-phase systems [18, 19], phase equilibrium of mixture [20-23] viscosity and thermal conductivity predictions of binary and ternary mixtures [24,25], polymer exchange membrane fuel cell performance [26-28], indicators of density functional theory metal hydride models[29], molar density and specific heat of water [30] and the liquid vapor pressure[31].

The main techniques used are represented by ANNs (which are mathematical representation of the working of the mammalian brain) and EAs (algorithms that apply the principle of evolution to determine a near optimum solution). The main reasons for the ANN popularity are their effectiveness, easiness of use, capability of modelling non-linear input-output relations and flexibility (as they can be applied to almost any type of process). Similarly, EAs are well-established techniques that can be efficiently applied where the classical optimization techniques fail or are too computationally expensive (require too much resources). The EAs are included into a larger class of algorithms called metaheuristic optimizers and in the latest years, a multitude of newer and better variants were proposed. Therefore, in this work, after the densities for the pure as well as binary mixtures of 1-pentanol or 1-decanol with 1,2-ethanediol or 1,2-propanediol or 1,3-butanediol or 2,3-butanediol were measured over the whole composition range at (288.15, 293.15, 298.15, 303.15, 308.15 and 313.15) K and at atmospheric pressure, an improved version of Bacterial Foraging Optimizer algorithm (which will be further called iBFO) is used to: i) determine the optimal values for the Spencer-Danner and Li equations for the considered system and ii) determine an alternative model for the system in the form of an ANN. Although ANNs are easy to apply and use, they are difficult to set up (determine the optimal architecture) and train (determine the optimal values for the internal parameters) and, in order to simplify this process, iBFO will perform a simultaneous parametric and structural optimization.

EXPERIMENTAL SECTION
Materials

All the chemicals were applied without additional purification and they were analytical grade. The chemical name,

Table 1: Specifications of the Used Chemicals.

Compound	Source	CAS NO	Molar mass g/mol (Supplier)	Purity (Supplier)	Water content [a] (supplier)	Water content (K.F) [b]
1-pentanol	Sigma-Aldrich	71-41-0	88.15	≥99.8%	≤0.002	0.00016
1-decanol	Sigma-Aldrich	112-30-1	158.28	≥99.5%	≤0.002	0.00034
1,2 ethanediol	Merck	107-21-1	62.07	≥99.5%	≤0.001	0.00025
1,2-propanediol	Merck	57-55-6	76.09	≥99.5%	≤0.001	0.00027
1,3-butanediol	Merck	107-88-0	90.12	≥99.2%	≤0.001	0.00018
2,3-butanediol	Merck	513-85-9	90.12	≥99.2%	≤0.002	0.00027

[a] *Purity stated by the supplier*

[b] *Determined by a microprocessor based automatic Karl–Fischer Titrated.*

CAS number (CAS), supplier, purity, and water content are shown in Table 1. Their water content mass fraction declared by the supplier were $\leq 2\times10^{-3}$. Also, to verify the accuracy of the analysis, Karl Fischer method (titrator model 751 GPD Titrino-Metrohm, Herisau, Switzerland) was used to determine the amount of water in pure alcohols. A good agreement between the supplier and Karl Fischer data was found.

Also, the purity of each pure liquids was checked indirectly by measuring the density and comparing it with the available literature values at all studied temperatures [32-51] (Table 1). Given the data from Table 2, the average Absolute Deviation Percent (ADD %) between experimental and literature values are between 0.000% for 1-decanol at T = 298.15 K [37] to maximum 0.37% for 1,2-ED at T = 303.15 and K [39] and the mean values of AAD% for all density values are equal to 0.17. Regarding the mean values of AAD%, a satisfactory agreement is found between the measured values in this work and the data reported in literature. Due to this good agreement, no further purification of all the materials used in this study were performed.

Experimental procedures

The preparation of the binary solutions was performed by adding the suitable mass of alkanol and alkanediol to 10g in 15 mL graded laboratory tubes, utilizing an analytical balance (A&D., Japan, model GF300) with an uncertainty of $\pm 10^{-4}$ g. Before measuring the density, the content of the test tubes was rigorously vortexed for 10 min to homogenize the solution; the tube was provided with an external jacket and put in a thermostatic bath (Member., Germany, model INE400) to keep the temperature constant within ± 0.1 K. To ensure complete miscibility, retention was allowed at a desired temperature for some hours. The Anton Paar oscillation U-tube densitometer (model DMA 500, Austria), calibrated with double- distilled water and air was used to measure the densities of pure liquids and their mixtures at different temperatures. The density values have a standard uncertainty of $\pm 10^{-4}$ g·cm^{-3}. All of these measurements were performed twice and the mean values were reported. Every effort was made to perform the measurements in the same day the solutions were prepared.

Modelling methodology
Spencer-Danner and Li equations

A number of investigators have developed equations for predicting the bubble-point density of mixtures.

Rackett [52] determined that saturated liquid volumes can be calculated by

$$V_s = V_c Z_c^{(1-\frac{T}{T_c})^{\frac{2}{7}}} \tag{1}$$

where $V_s =$ saturated liquid volume, $V_c =$ critical volume, $Z_c =$ critical compressibility factor, $T_c =$ critical temperature. Equation (1) is often written in the equivalent form

$$V_s = \frac{R T_c}{P_c} Z_c^{\left[1+\left(1-\frac{T}{T_c}\right)^{\frac{2}{7}}\right]} \tag{2}$$

While equation (1) is remarkably accurate for many substances, it underpredicts V_s when $Z_C < 0.22$.

Yamada and Gunn [53] indicated that Zc in Eq. (1) can be correlated with the acentric factor (ω):

$$V_s = V_c (0.29056 - 0.08775\omega)^{(1-\frac{T}{T_c})^{\frac{2}{7}}} \tag{3}$$

Table 2: Densities ρ, of the pure components studied in this work at various temperatures T and pressure of 0.1 MPa[a].

Material	T/K	$10^{-3} \times \rho$/g.cm^{-3}		
		Exp.	Lit.	AAD%[b]
1-pentanol	288.15	0.8200	-	-
	293.15	0.8162	0.8147[32]	0.18
	298.15	0.8123	0.8111 [33]	0.15
			0.81094[34]	0.17
			0.81112[35]	0.15
	303.15	0.8085	0.8073[32]	0.15
	308.15	0.8048	0.8037 [33]	0.14
			0.80352[34]	0.16
			0.80345[36]	0.17
	313.15	0.8012	0.7998[32]	0.18
1-decanol	288.15	0.8333	-	-
	293.15	0.8298	-	-
	298.15	0.8264	0.826388[37]	0.00
		0.8229	0.822970[37]	0.01
	303.15	0.8195	0.819534[37]	0.03
	308.15	0.8160	-	-
		0.8333	-	-
	313.15	0.8298	-	-
1,2-Ethanediol	298.15	1.1062	1.1097 [38]	0.32
			1.1098 [39]	0.33
			1.1102 [40]	0.36
			1.1097 [41]	0.32
			1.1098 [42]	0.33
			1.1095 [43]	0.30
	303.15	1.1027	1.10294 [44]	0.02
			1.1068 [39]	0.37
			1.1067 [40]	0.36
			1.1062 [41]	0.32
			1.1064 [42]	0.34
			1.1054 [43]	0.24
	308.15	1.0992	1.1032 [39]	0.36
			1.1029 [42]	0.33
	313.15	1.0957	1.0998 [39]	0.37
			1.09923 [42]	0.32
			1.09907 [41]	0.31

Table 2: Densities ρ, of the pure components studied in this work at various temperatures T and pressure of 0.1 MPa^a. (Continuation)

Material	T/K	$10^{-3} \times \rho / g.cm^{-3}$		
		Exp.	Lit.	AAD%[b]
1,2-Propanediol	298.15	1.0332	1.03286 [39]	0.03
			1.03286 [41]	0.03
			1.03277 [45]	0.04
			1.032588 [46]	0.06
			1.03283 [47]	0.04
	303.15	1.0294	1.02915 [39]	0.02
			1.0291 [41]	0.03
			1.028881 [46]	0.05
			1.02902 [47]	0.04
	308.15	1.0257	1.02557 [39]	0.01
			1.0254 [45]	0.03
			1.025088[48]	0.07
	313.15	1.0219	1.02144 [40]	0.05
			1.02148 [41]	0.04
			1.021300[48]	0.06
1,3-Butanediol	298.15	1.0033	1.00003 [45]	0.33
			1.0000 [47]	0.33
	303.15	1.0001	-	-
	308.15	0.9968	0.99422 [45]	0.26
			0.99420 [49]	0.26
	313.15	0.9939	-	-
2,3-Butanediol	288.15	1.0073	1.0055[50]	0.18
	293.15	1.0034	1.0033[51]	0.01
	298.15	0.9996	0.9984[50]	0.12
			0.99857[45]	0.10
	303.15	0.9956	-	-
	308.15	0.9916	0.9908[50]	0.08
			0.99211[45]	0.05
	313.15	0.9877	-	-

^{a}*Standard uncertainties are (x_i) = 0.0001, u (ρ) = 0.0001 $g.cm^{-3}$, u (n_D) = 0.0001, u (η) =0.002 and u (T) = 0.05 K*

$^b(ADD\%) = \frac{100}{N} \sum_{i=1}^{N} \left| \frac{A_i^{exp} - A_i^{cal}}{A_i^{exp}} \right|$ *, where N denotes the number of experimental data points.*

In order to extend equations to predict the density of mixtures such as Eq. (3) to mixtures, mixing rules are required. *Li* [7, 54] and *Spencer* and *Danner* [7, 9] indicated that Eq.4, which is an extension of the Rackett equation, will give an accuracy equivalent to any available methods.

$$V_m = R \left(\sum_i \frac{x_i T_{ci}}{P_{ci}} \right) Z_{RAm}^{[1+(1-T_r)^{0/2857}]} \tag{4}$$

$$Z_{RAm} = \sum x_i Z_{RAi} \tag{5}$$

With the relation of Yamada and Gunn [49]

$$Z_{RAi} = 0/29056 - 0/08775 \omega_i \tag{6}$$

Where $T_r = \frac{T}{T_{cm}}$. *Spencer* and *Danner* [7, 9] recommend the mixing rules of *Chueh* and *Prausnitz* [7,55].

$$T_{cm} = \sum_i \sum_j \emptyset_i \emptyset_j T_{cij} \tag{7}$$

$$\emptyset_i = \frac{x_i V_{ci}}{\sum_j x_j V_{cj}} \tag{8}$$

$$1 - k_{ij} = \frac{8(V_{ci} V_{cj})^{1/2}}{\left(V_{ci}^{1/3} + V_{cj}^{1/3}\right)^3} \tag{9}$$

$$T_{cij} = (1 - k_{ij})(T_{ci} T_{cj})^{1/2} \tag{10}$$

Li's method sets $K_{ij} = 0$ for Eq. (10) [7, 9].

Artificial Neural Networks

The ANNs are inspired from the biological brain. They are formed from artificial neurons organized in layers. The manner in which the layers are connected indicate the type of the ANN. The most known and used type of ANN is represented by the Feed Forward Multilayer Perceptron Neural Network (MLP), where the neurons in each layer are fully connected with all the neurons in the next layer and the signal is transmitted in a single direction, from inputs to outputs. A schema of a general MLP with one hidden layer is presented in Fig. 1, where *In* represents the input, $w_{i,j}$ the weight from neuron i to neuron j, N_k represents the k neuron from the hidden layer and N_{outi} the ith neuron from the output layer, b_i and af_i the bias and the activation function on the ith neuron. In the majority of frameworks implementing ANNs, the activation function is specified by layer, which means that all the neurons in the same layer have the same type of activation function. However, in this work, the activation function is considered as being specific to each neuron

In order for an ANN to be applied to a specific problem, its optimal structure must be determined and a training phase performed. The number of inputs and outputs of an ANN depends on the characteristics of the problem being solved. On the other hand, the number of hidden layers and of neurons in each hidden layer is dependent on the complexity of the relations between inputs and inputs and on the available number of data describing the system being modeled. The higher the number of hidden layers and neurons the higher the number of weights that must be determined in the training phase.

In the training phase, the optimal values of the weights and biases are determined so that the lowest error between the available data and the predicted values is obtained. There are different types of training (supervised, unsupervised and semi-supervised) and from the supervised category, the BackPropagation algorithm is the most known. It is based on a generalization of the Widrow-Hoff learning rule [56] and it suffers from all the problems characteristic to the steepest descent approaches. In order to eliminate this problem, in this work, the topology determination and training is simultaneously performed using a bio-inspired metaheuristic represented by iBFO.

Optimization procedure

In order to optimize the models of the considered system (the Spencer-Danner and Li equations and the ANN), in this work, a new improved version of Bacterial Foraging Optimization algorithm is applied. The standard version of the optimizer will be referred as BFO and the novel variant proposed in this work as iBFO. BFO was proposed in 2002 by [57] and it is inspired from the foraging behavior of *Escherichia coli* bacteria. It simulates the foraging concept at colony level rather at individual level and includes behaviors such as chemotaxis, reproduction, elimination and dispersal (Fig. 2) [58]. The terminology used in the initial BFO variant indicates the bacterium as the structure that forms the colony. As it was pointed out by many researchers [58-61], the terminology specific to each metaheuristic can be confusing and difficult to understand and therefore, in order to simplify it and to keep it on the same level as the one used in the EA field, the bacterium will be further referred as 'individual' and the colony as 'population'.
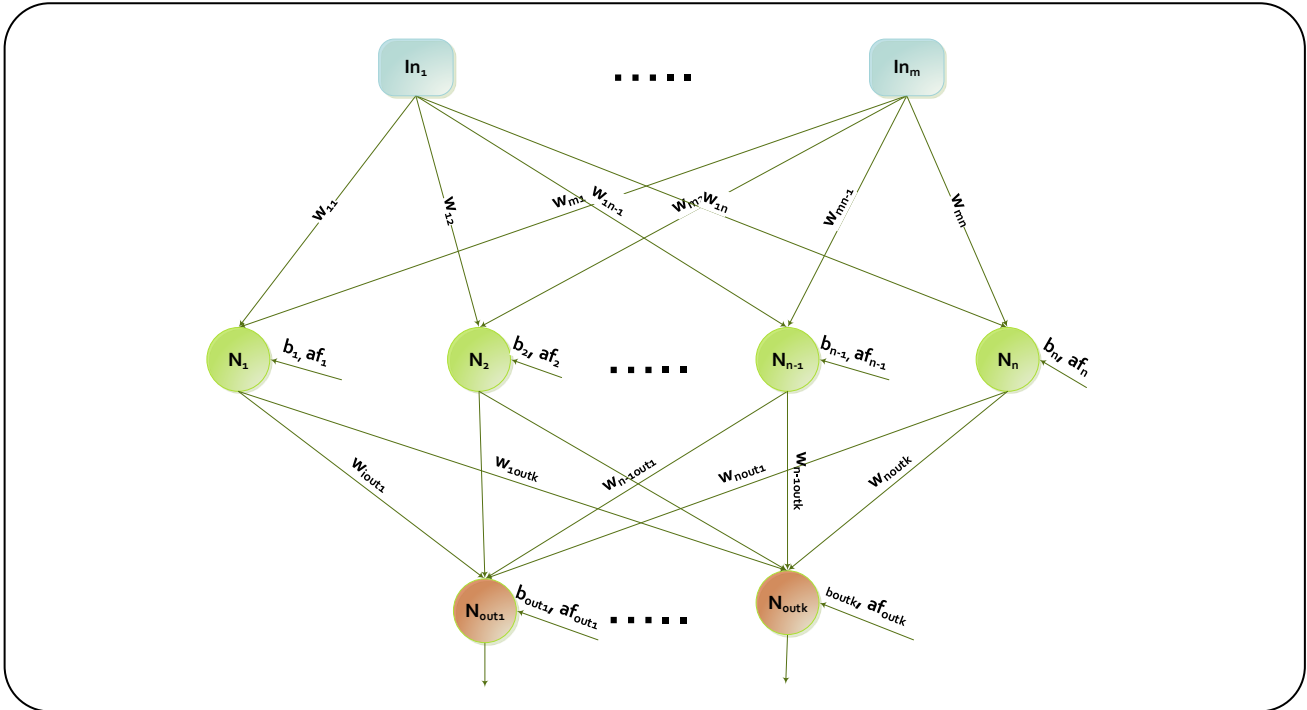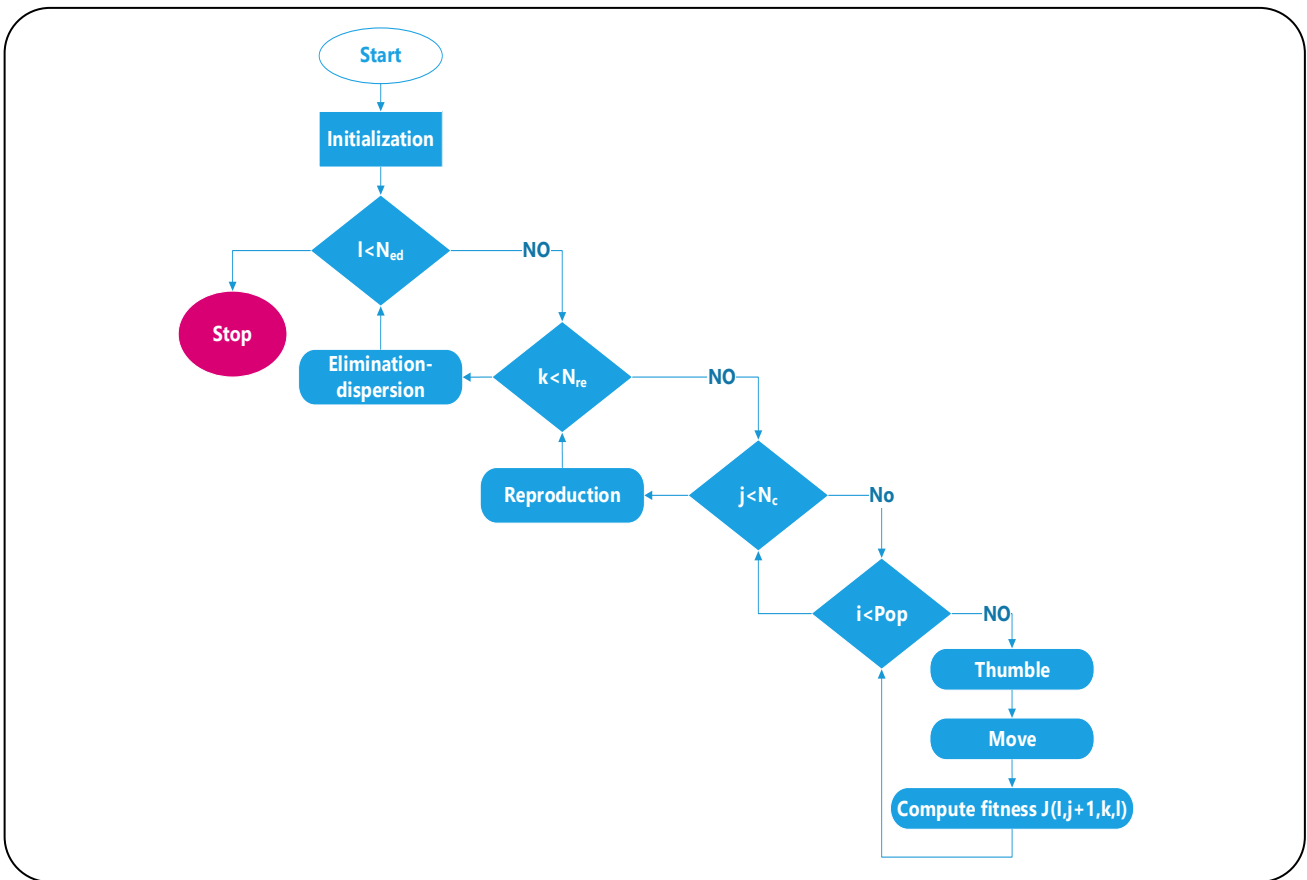
Fig. 1: General schema of an MLP neural network.

Fig. 2: Simplified schema of the BFO algorithm.

Based on the perceived chemical gradients from the environment the bacteria rotate their flagella to move: i) a clockwise rotation causes a forward movement -known as move or swim-(which is performed when a rich gradient is reached); ii) a counterclockwise rotation generates a tumbling effect that causes a movement in a random direction (which is performed when searching for a richer gradient zone). These two types of movement represent the bacterial chemotaxis. The life-time of the individual is measured by the number of chemotactic steps it takes (represented by Nc)

In the reproduction step, the 50% healthiest bacteria (a measure of how many nutrients found and how successful it was at avoiding noxious substances - aspect indicated by the fitness function J -) are split into two identical individuals. The created copies replace the less healthy individuals. The reproduction step is repeated Nre times.

In the elimination-dispersal step, with a p_{ed} probability, the individuals are removed from the population and replaced with newly generated individuals. This step is repeated N_{ed} times. As p_{ed} is fixed, the healthy and the least heaty individuals have the same probability of being replaced. Therefore, there can be cases where individuals located in the vicinity of the global optimum are replaced with individuals far from the optimum. In order to avoid this aspect, and to allow exploration when in the population are preponderantly less healthy individuals and exploitation when there are more healthy individuals, the p_{ed} is modified adaptively (Eq. 11). This modification represents the main idea of the iBFO variant.

$$p_{ed} = \tag{11}$$
$$\begin{cases} \dfrac{fit_{min} + fit_{avg}}{fit_{max} + fit_{min}}, if\ the\ objective\ is\ fitness\ minimization \\ \dfrac{fit_{max} - fit_{avg}}{fit_{max} - fit_{min}}, if\ the\ objective\ is\ fitness\ maximization \end{cases}$$

where fit_{min} represents the minimum of the fitness of all individuals, fit_{max} the maximum and fit_{avg} the average.

The modified BFO version is then used to optimize the: i) Spencer-Danner equation; ii) Li equation; iii) the ANN model. In the first and second case, the free parameters of the equations represent the parameters that are included into the individuals forming the population. In the third case, a direct encoding is used to transform the ANN into a vector with real numbers. It contains the following data: number of hidden layers, number of neurons in each hidden layer, weights, biases, activation functions and their parameters.

RESULTS AND DISCUSSION
Experimental analysis

The experimental data of density (ρ) and the calculated density by Spencer-Danner and Li equations and ANN model for seven binary liquid mixtures {(1-pentanol + 1,2-ethanediol), (1-pentanol+ 1,2-propanediol), (1-pentanol+ 1,3-butanediol), (1-pentanol + 2,3-butanediol), (1-decanol + 1,2-propanediol), (1-decanol + 1,3-butanediol) and (1-decanol + 2,3-butanediol)} at six temperatures (T = 288.15, 293.15, 298.15, 303.15, 308.15 and 313.15) K over the entire concentration range and atmospheric pressure are reported in Table S1. According to Table S1 and Figs. S1-S7, as the alkanol concentration increases, the density decreases. On the other hand, in this study, the density of pure alkanols is lower than that of alkanediols, and increasing the concentration of alkanol in the binary system of alkanol + alkanediols reduces the density of the mixture. Also, increasing temperature has led to a decrease in density. The weakening of the intermolecular bonding strength and of the attraction between like and unlike molecules is a result of the extension of molecular agitation at higher temperatures. Consequently, the solution density is reduced and the total volume of mixture is expanded.

Spencer-Danner and Li equations

After applying the Spencer-Danner and Li equations the average absolute error (AAD%) compared with the experimental data are 26.31% and 26.51%. For the Spencer-Danner equation the absolute error (AD) varies from 0.015% to 72.77% and for Li equation from 2.8E-05% to 73.11%. This high variation indicates that these equations do not always manage to capture the differences between the characteristics of mixture and to efficiently predict the density. As these equations have free parameters (fixed numerical values that do not have a physical correlation), in order to correct the models, these parameters were included into iBFO and optimized in order to reduce the AAD between the predicted values and the experimental data. The simulations were performed using the standard values for the control parameters of BFO (which are also the control parameters of iBFO): N_c=20, N_s=5, N_{re}=8, N_{ed}=20, and intial value for p_{ed}=0.25. These values were used in all the simulations performed with iBFO for both model correction and ANN model optimization. In case of model correction, the iBFO was implemented for fitness maximization, where the fitness function is defined as:

Table 3: Optimization results for the Spencer-Danner equation.

No crt.	Z_{RAi} param no 1	Z_{RAi} param no 2	$1-k_{ij}$ param	V_m param	MSE	Fitness
1	0.204524	0.000341	7.75803	0.856625	0.002618155	381.9483721
2	0.169122	0.005636	8.162955	1.467956	0.002812363	355.5729034
3	0.209740	0.002489	8.175595	0.841681	0.002877584	347.5137405
4	0.211684	0.004525	9.011792	0.832806	0.002925056	341.8737606
5	0.182087	0.003091	9.694200	1.347853	0.003205429	311.9706970
6	0.156847	0.011477	7.703689	1.783278	0.003326817	300.5875815
7	0.204269	0.010489	9.076000	1.019896	0.003363206	297.3353804
8	0.101698	0.009995	10.56756	5.073863	0.004210575	237.4972808
9	0.134288	0.011250	9.225008	2.501052	0.004593001	217.7225798
10	0.267646	0.016471	9.651160	0.326427	0.004664778	214.3724624

$$\text{Fitness} = \frac{1}{\text{MSE}} \tag{12}$$

Where *MSE* represent the mean squared error between the predictions and the experimental values computed for the entire dataset for which experimental data were determined.

As iBFO is a stochastic optimization approach and relies on randomization, the algorithm was run 10 times, with a stop condition representing by the number of function valuations (number of times the fitness function was computed) of 1.0E+06.

In the optimization procedure, for the Spencer-Danner equation, the following parameters were optimized: the parameters included in the determination of Z_{Rai} (initial values 0.29056 and 0.08775), the parameter included in the calculation of $1-k_{ij}$ (initial value 8) and the parameter included in the calculation of V_m (initial value 0.2857). The results obtained (order based on the performance from highest to lowest) are presented in Table 3.

For the best solution from Table 3 (No crt 1), the AAD decreased to 3.51%, with a variation of the AD from 0.013% to 17.85%

For the Li equation, the following parameters were optimized: the parameters included in the determination of Z_{Rai} (initial values 0.29056 and 0.08775) and the parameter included in the calculation of V_m (initial value 0.2857). The results obtained (order based on the performance from highest to lowest) are presented in Table 4.

For the best solution from Table 4 (No crt 1), the AAD decreased to 4.01%, with a variation of the AAD from 0.003% to 17.72%.

As it can be observed, by optimizing the equations free parameters, the AAD is drastically reduced, the error reaching lower values. These results indicate the capability of iBFO to perform optimization of various subcomponents so that low errors between predictions and experimental are obtained.

Artificial Neural Networks (ANN)

Along the Spencer-Danner and Li equations, the considered system was also modeled using an alternative approach in the form of ANNs. In order to obtain a good ANN model, first the data underwent a set of pre-processing steps that include: randomization (so as the data to be randomly included in the training or testing sub-sets), normalization (to reduce the influence of high value inputs) using a min-max approach [62] and data assignation (into training -75% of exemplars- and testing -the remaining 25%- sub-sets).

After that, the iBFO was applied to determine the optimal ANNs. In this case, the same iBFO parameters used for the optimization of Spencer-Danner and Li equations were employed. As the number of parameters considered for optimization is much higher compared to the previous case, a limitation on the maximum allowed topology was set: maximum number of hidden layer 2, maximum neurons in the first hidden layer: 20, maximum neurons in the second hidden layer:10. The ANN has 4 inputs (corresponding to temperature, alkanol concentration, alkanol molecular weight and alkanediol

Table 4: Optimization results for the Li equation.

No crt	Z_{RAi} param no 1	Z_{RAi} param no 2	V_m param	MSE	Fitness
1	0.166713	0.00067	1.457327956	0.002586682	386.5956
2	0.193836	0.000416	1.034027956	0.002727195	366.6771
3	0.15983	0.003492	1.620231655	0.002775955	360.2364
4	0.165345	0.003264	1.533459795	0.002801394	356.9651
5	0.198458	0.002037	0.985590575	0.002817168	354.9664
6	0.192694	0.001439	1.065100418	0.002819783	354.6372
7	0.226237	0.006498	0.636168734	0.003054998	327.3324
8	0.235863	0.007655	0.606152104	0.004406578	226.9335
9	0.266095	0.009367	0.281260577	0.004442773	225.0847
10	0.162044	0.02338	1.823999516	0.006401154	156.2218

Table 5. Statistics for the ANN models

	Fitness	MSE train	MSE test	Correlation train	Correlation test	Topology
Best	21743.56	4.6E-05	0.000176	0.97551	0.962772	4:10:01
Worst	1086.939	0.00092	0.002214	0.164367	0.250787	4:13:01
Average	5103.41	0.000331	0.000994	0.793677	0.767167	

molecular weight) and 1 output; in combination with the previously mentioned limitations, the individual encoding the ANN has the following length: 1 (1 parameter indicating the number of hidden layers: {0,1, or 2}) + 1(1 parameter for the number of neurons in the first hidden layer:{0,1,2,..,20}) + 1 (1 parameter for the number of neurons in the second hidden layer) + 4x20+20x10+10x1 (110 weights)+ 20+10+1(31 biases) + 20+10+1 (31 activation functions)+20+10+1(31 parameters of the activation functions)= 206.

In order to determine the best ANN model, the number of simulations performed in this case is 50. The statistics for the determined models are presented in Table 5. Because in this case there are 2 subsets of data, the fitness function is modified as follows:

$$Fitness = \frac{1}{MSE_{training} + 10^{-10}} \qquad (13)$$

Where $MSE_{training}$ indicates the MSE for the training subset.

As it can be observed from Table 5, the best obtained ANN has a topology with a single hidden layer and 10 neurons in the hidden layer. The AAD for the training subset is 1.36% and for testing subset 1.49%. For the overall dataset, the AAD is 1.4 % (with a minimum AD of 0.001% and a maximum AD of 8.27%). Compared with the modified forms of the Spencer-Danner and Li equations, the best ANN model determined (Eqs (14-29)) is better but more complex.

$$INP\_1 = -1.0000 - 1e - 10 + \qquad (14)$$

$$2.0000 \times (T - 288.15)/(313.15 - 288.15)$$

$$INP\_2 = -1.0000 - 1e - 10 + \qquad (15)$$

$$2.0000 \times (Xa - 0.0507)/(0.9804 - 0.0507)$$

$$INP\_3 = -1.0000 - 1e - 10 + \qquad (16)$$

$$2.0000 \times (Ma - 88.15)/(158.28 - 88.15)$$

$$INP\_4 = -1.0000 - 1e - 10 + \qquad (17)$$

$$2.0000 \times (Mb - 62.07)/(90.12 - 62.07)$$

$$IHl\_0 = (+INP\_0 \times 0.538014112464014 + \tag{18}$$
$$INP\_1 \times 2.71566633152776 +$$
$$INP\_2 \times 0.803561140842874 +$$
$$INP\_3 \times -0.0664251837688311 +$$
$$1.35534724571033)$$

$$Hl\_1 = (1.0 \ / \ (1.0 + \tag{19}$$
$$\exp(-(+INP\_0 \times -0.117986596550717 +$$
$$INP\_1 \times 1.87839318174615 +$$
$$INP\_2 \times 0.650681567436466 +$$
$$INP\_3 \times -3.34518406315425 +$$
$$-2.16745152474951))))$$

$$Hl\_2 = (1.0 / (1.0 + \tag{20}$$
$$\exp(-0.985180555517293 \times$$
$$(+INP\_0 \times -0.0494079462154517 +$$
$$INP\_1 \times -1.99968895840127 +$$
$$INP\_2 \times -2.697790117038 +$$
$$INP\_3 \times -3.07806777564342 +$$
$$3.20915523273081))))$$

$$Hl\_3 = (1.0 / (1.0 + \tag{21}$$
$$\exp(-(+INP\_0 \times -1.13552239818899 +$$
$$INP\_1 \times -2.59589242769507 +$$
$$INP\_2 \times -3.31694888362031 +$$
$$INP\_3 \times -0.595717943747883 +$$
$$-1.04619704303432))))$$

$$Hl\_4 = (2.0 / (1.0 + \tag{22}$$
$$\exp(-2 \times (+INP\_0 \times 2.62566290648349 +$$
$$INP\_1 \times 3.85614059888569 +$$
$$INP\_2 \times -2.94792472325152 +$$
$$INP\_3 \times 1.89131164445573 +$$
$$2.3630564218857))) - 1.0)$$

$$Hl\_5 = \exp(-pow(-(+INP\_0 \times 0.607151301538788 + \tag{23}$$
$$INP\_1 \times -1.90991380689639 +$$
$$INP\_2 \times 0.863834750606748 +$$
$$INP\_3 \times 1.25296449104419 +$$
$$-1.88815807423083), 2.0))$$

$$Hl\_6 = (1.0 \ / \ (1.0 + \tag{24}$$
$$\exp(-(+INP\_0 \times 2.27173161865399 +$$
$$INP\_1 \times -3.76195560911522 +$$
$$INP\_2 \times -2.28427320350572 +$$
$$INP\_3 \times -0.25441574183084 +$$
$$-1.26406086588109))))$$

$$Hl\_7 = (2.0 / (1.0 + \tag{25}$$
$$\exp(-2 \times (+INP\_0 \times 2.14280728434223 +$$
$$INP\_1 \times 1.6011577842267 +$$
$$INP\_2 \times -1.13694068679597 +$$
$$INP\_3 \times 0.845855533503027 +$$
$$-1.40399558625801))) - 1.0)$$

$$Hl\_8 = \exp(-pow(-(+INP\_0 \times -1.20860700239875 + \tag{26}$$
$$INP\_1 \times -2.74363607876265 +$$
$$INP\_2 \times -2.09041587369404 +$$
$$INP\_3 \times 1.0159125664968 + -$$
$$3.45086144383626), 2.0))$$

$$Hl\_9 = (1.0 / (1.0 + \tag{27}$$
$$\exp(-(+INP\_0 \times -1.55042454691944 +$$
$$INP\_1 \times -0.714634298871562 +$$
$$INP\_2 \times -1.27726298787646 +$$
$$INP\_3 \times 1.98641997329205 +$$
$$-2.1796052102893))))$$

$$OUTPUT\_1 = (2.0 / (1.0 + \tag{28}$$
$$\exp(-0.132428129987276 \times$$
$$(+Hl\_0 \times -3.95041356616667 +$$
$$Hl\_1 \times -1.28208530732835 +$$
$$Hl\_2 \times -0.474192546177217 +$$
$$Hl\_3 \times -1.91287622310382 +$$
$$Hl\_4 \times -1.60193068396212 +$$
$$Hl\_5 \times 2.05918838612152 +$$
$$Hl\_6 \times 3.31895724919471 +$$
$$Hl\_7 \times -1.16028774639627 +$$
$$Hl\_8 \times -0.507902693082274 +$$
$$Hl\_9 \times 1.1733834253948 +$$
$$-1.92145738578373))) - 1.0)$$

$$Density = \frac{(OUTPUT\_1 + 1.0000 + 1e - 10) \times (1.0738 - 0.8036)}{2.0000 + 0.8036} \tag{29}$$

CONCLUSIONS

The new experimental densities for the pure as well as binary mixtures of 1-pentanol or 1-decanol with 1,2-ethanediol or 1,2-propanediol or 1,3-butanediol or 2,3-butanediol were measured over the whole composition range at (288.15, 293.15, 298.15, 303.15, 308.15 and 313.15) K and at normal atmospheric pressure. For this system, two types of modeling were performed: phenomenological, represented by Spencer-Danner and Li equations and black-box, represented by Artificial Neural Networks (ANN).

The classical relation for the Spencer-Danner and Li equations used for determining the density did not provide acceptable results, so an improved Bacterial Foraging Optimization algorithm was applied to correct the free parameters. The improvement consisted of introducing an adaptive strategy for changing the probability of replacing individuals with newly generated ones based on the average fitness of the entire population. The optimization results showed that the Spencer-Danner and Li equations were improved, the ADD% being reduced from 26.31% to 3.51% and from 26.51% to 4.0001% respectively. These substantially improved results proved that iBFO can lead to optimized models that can be further used for density predictions.

In the case of black-box modeling, the same iBFO algorithm was applied to automatically determine the internal parameters and structure. For the resulting ANN model, the overall ADD was 1.4%, significantly lower than the optimized phenomenological models. These results prove the efficiency of Artificial Intelligence based techniques to capture the system dynamic and to generate highly performant models. Although having the best performance, the ANN is more complex than the optimized phenomenological models and it is suitable when the computational resources are not limited (as in the case of microchip processing).

Acknowledgments

REFERENCES

[1] Ge M.L., Ma J-L., Chu B., Densities and Viscosities of Propane-1,2,3-Triol + Ethane-1,2-Diol at T(298.15 to 338.15) K, *J. Chem. Eng. Data*, **55(1)**: 2649–2651 (2010).

[2] Pimentel-Rodas A., Galicia-Luna L.A., Castro-Arellano J.J., Simultaneous Measurement of Dynamic Viscosity and Density of n-Alkanes at High Pressures, *J. Chem. Eng. Data.*, **62(1)**: 3946-3957 (2017).

[3] Pimentel-Rodas A., Galicia-Luna L.A., Castro-Arellano J.J., Viscosity and Density of N Alcohols at Temperatures Between (298.15 and 323.15) K and Pressures up to 30 MPa, *J. Chem. Eng. Data.* **64(1)**: 324-336 (2019).

[4] Zorębski E., Lubowiecka-Kostka B., Thermodynamic and Transport Properties of (1,2-Ethanediol + 1-Nonanol) at Temperatures from (298.15 to 313.15) K, *J. Chem. Thermodyn.* **41(1)**: 97–204 (2009).

[5] Doghaei A.V., Rostami A.A., Omrani A., Densities, Viscosities, and Volumetric Properties of Binary Mixtures of 1,2-Propanediol + 1-Heptanol or 1-Hexanol and 1,2-Ethanediol + 2-Butanol or 2-Propanol at T(298.15, 303.15, and 308.15) K, *J. Chem. Eng. Data.* **55(1)**: 2894–2899(2010).

[6] Kermanpour F., Niakan H. Z., Sharifi T., Density and Viscosity Measurements of Binary Alkanol Mixtures from (293.15 to 333.15) K at Atmospheric Pressure, *J. Chem. Eng. Data.* **58(1)**: 1086-1091(2013).

[7] Poling B.E., Prausnitz J.M., O'Connell J.P., "The Properties of Gases and Liquids", 5th ed, McGraw-Hill Education (2001).

[8] Spencer C.F., Danner R.P., Improved Equation for Prediction of Saturated Liquid Density, *J. Chem. Eng. Data.*, **17(1)**: 236-241(1972).

[9] Spencer C.F., Danner R.P., Prediction of Bubble-Point Density of Mixtures, *J. Chem. Eng. Data.* **18(1)**: 230-234 (1973).

[10] Spencer C.F., Adler S.B., A Critical Review of Equations for Predicting Saturated Liquid Density, *J. Chem. Eng. Data.* **23(1)**: 83-89(1978).

[11] Mohsen-Nia M., Modarress H., Rasa H., Measurement and Modeling of Density, Kinematic Viscosity, and Refractive Index for Poly(Ethylene Glycol) Aqueous Solution at Different Temperatures, *J. Chem. Eng. Data.*, **50(1)**:1662-16662005.

[12] Jouyban A., Mirheydari S.N., Barzegar-Jalali M., Shekaari H., Acree J.W.E., Comprehensive Models for Density Prediction of Ionic Liquid +Molecular Solvent Mixtures at Different Temperatures, *Phys. Chem. Liquids*, **58(3)**: 309-324 (2020).

[13] Pirdashti M., Curteanu S., Kamangar M.H., Hassim M.H., Khatami M.A., Artificial Neural Networks: Applications in Chemical Engineering, *Rev. Chem. Eng.*, **29(4)**: 205-239 (2013).

[14] Lombardi C., Mazzola A., Prediction of Two-Phase Mixture Density Using Artificial Neural Networks, *Ann. Nuc. Energy*, **24(17)**: 1373-1387(1997).

[15] Rocabruno-Valdés C.I., Ramírez-Verduzco L.F., Hernández J.A., Artificial Neural Network Models to Predict Density, Dynamic Viscosity, and Cetane Number of Biodiesel, *Fuel*, **147(1)**: 9-17 (2015).

[16] Najafi-Marghmaleki A., Khosravi-Nikou M.R., Barati-Harooni A., A New Model for Prediction of Binary Mixture of Ionic Liquids+ Water Density Using Artificial Neural Network, *J. Mol. Liq.* **220(1)**: 232-237(2016).

[17] Najafi-Marghmaleki A., Khosravi-Nikou M.R., Barati-Harooni A., A New Model for Prediction of Binary Mixture of Ionic Liquids + Water Density Using Artificial Neural Network, *J Mol Liq.,* **220(1)**; 232-237 (2016).

[18] Qi G.H., Dong F., Xu V.B., Wu M.M., Hu J., Gas/Liquid Two-Phase Flow Regime Identification in Horizontal Pipe Using Support Vector Machines, *International Conference on Machine Learning and Cybernetics*, 1746-1751(2005).

[19] Wang L., Liu J., Yan Y., Wang X., Wang T., Gas-Liquid Two-Phase Flow Measurement Using Coriolis Flowmeters Incorporating Artificial Neural Network, Support Vector Machine, and Genetic Programming Algorithms, *IEEE Trans Instrum Meas*, **66(5)**: 852-868 (2017).

[20] Pirdashti M.., Movagharnejad K., Curteanu S., Dragoi E.N., Rahimpour F., Prediction of Partition Coefficients of Guanidine Hydrochloride in PEG–Phosphate Systems Using Neural Networks Developed with Differential Evolution Algorithm, *J. Ind. Eng. Chem.*, **27(1)**: 268-275 (2015).

[21] Pirdashti M., Movagharnejad K., Curteanu S., Leon F., Rahimpour F., LLE Data Prediction Using the K-Nearest Neighbor Method, *Iran. J. Chem. Eng.*, **13(1)**: 14-32 (2016).

[22] Pirdashti M.., Movagharnejad K., Mobalegholeslam P., Curteanu S., Leon F., Phase Equilibrium and Physical Properties of Aqueous Mixtures of Poly (vinyl pyrrolidone) with Trisodium Citrate, Obtained Experimentally and by Simulation, *J. Mol. Liq.,* **223(1)**: 903-920(2016).

[23] Pirdashti M., Taheri M., Dragoi E-N., Curteanu S., Machine Learning Approaches for Prediction of Phase Equilibria in Poly (Ethylene Glycol) + Sodium Phosphate Aqueous Two-Phase Systems, *Iran. J. Chem. Chem. Eng. (IJCCE),* **39(6)**: 185-197 (2020).

[24] Lashkarblooki M., Hezave A.Z., AL-Ajami A.M., Ayatollahi S., Viscosity Prediction of Ternary Mixtures Containing ILs Using Multi-Layer Perceptron Artificial Neural Network, *Fluid Phase Equilib.*, **326(1)**: 15-20 (2012).

[25] Shahsavar A., S Khanmohammadi., Karimipour A., Goodarzi M., A Novel Comprehensive Experimental Study Concerned Synthesizes and Prepare Liquid Paraffin-Fe3O4 Mixture to Develop Models for Both Thermal Conductivity & Viscosity: A New Approach of GMDH Type of Neural Network, *Int. J. Heat Mass Tran.*, **131(1)**: 432-441(2019).

[26] Melo E.B., Oliveira E.T., Martins T.D., Artificial Neural Network Prediction Indicators of Density Functional Theory Metal Hydride Models, *Fluid Phase Equilib.*, **506(1)**: 112411 (2021)

[27] Griffin W.O., Darse J.A., A Neural Network Correlation for Molar Density and Specific Heat of Water: Predictions at Pressures up to 100 MPa, *Int. J. Hydrog.*, **38(27)**: 11920-11929 (2013).

[28] Tarjomannejad A., Prediction of the Liquid Vapor Pressure Using the Artificial Neural Network-Group Contribution Method, *Iran. J. Chem. Chem. Eng. (IJCCE)*, **34(4)**: 97-111 (2015).

[29] Ahmadi N., Rezazadeh S., Dadvand A., Mirzaee I., Numerical Investigation of the Effect of Gas Diffusion Layer with Semicircular Prominences on Polymer Exchange Membrane Fuel Cell Performance and Species Distribution, *Int. J. Sustain. Energy*, **2(2)**: 36-46 (2015).

[30] Ahmadi N., Kõrgesaar M., Analytical Approach to Investigate the Effect of Gas Channel Draft Angle on the Performance of PEMFC and Species Distribution. *Int. J. Heat Mass Transf.,* **152(1)**: 119529 (2020).

[31] Ahmadi N., Rezazadeh S., Asgharikia M., Shabahangnia E., Optimization of Polymer Electrolyte Membrane Fuel Cell Performance by Geometrical Changes. *Iran. J. Chem. Chem. Eng.*, *(IJCCE)*, **36(2)**: 89-106 (2017).

[32] Boned Ch., Baylaucq A., . Bazile J.P. Liquid Density of 1-Pentanol at Pressures up to 140 MPa and from 293.15 to 403.15 K, *Fluid Phase Equilib*. **270**(1-2): 69-74 (2008).

[33] Srinivasa R., Imran Khan M., Thomas K., Raju S.S., Suresh P., Hari Babu B., The Study of Molecular Interactions in 1-Ethyl-3-methylimidazolium Trifluoromethanesulfonate+ 1-Pentanol from Density, Speed of Sound and Refractive Index Measurements, *J. Chem. Thermodyn*. **98(1)**: 298-308 (2016).

[34] Urszula D., Laskowska M.. Effect of Temperature and Composition on the Density and Viscosity of Binary Mixtures of Ionic Liquid with Alcohols, *J. Sol Chem*. **38(1)**: 779-799(2009).

[35] Almasi M., Mousavi L., Excess Molar Volumes of Binary Mixtures of Aliphatic Alcohols (C1–C5) with Nitromethane over the Temperature Range 293.15 to 308.15 K: Application of the ERAS Model and Cubic EOS, *J. Mol. Liq.* **163**(1): 46-52 (2011).

[36] Al-Jimaz S., Adel A., Al-Kandary J., Abdul-Latif A.M., Densities and Viscosities for Binary Mixtures of Phenetole with 1-Pentanol, 1-Hexanol, 1-Heptanol, 1-Octanol, 1-Nonanol, and 1-Decanol at Different Temperatures, *Fluid Phase Equilib*., **218(1)**: 247-260 (2004).

[37] Estrada-Baltazar A., Bravo-Sanchez M.G., Iglesias-Silva G.A., Alvarado J.F.J., Castrejon-Gonzalez, Ramos-Estrada E.O. M., Densities and Viscosities of Binary Mixtures of n-Decane+ 1-Pentanol,+ 1-Hexanol,+ 1-Heptanol at Temperatures from 293.15 to 363.15 K and Atmospheric Pressure, *J. Chem. Eng.* **23(1)**: 559-571 (2015).

[38] Moosavi M., Motahari A., Rostami A.A., Investigation on Some Thermophysical Properties of Poly(ethylene glycol) Binary Mixtures at Different Temperatures, *J. Chem. Thermodyn*. **58(1)**: 340–350 (2013).

[39] Li Q.S., Tian Y.M., Vang S., Densities and Excess Molar Volumes for Binary Mixtures of 1,4-Butanediol + 1,2-Propanediol, + 1,3-Propanediol, and + Ethane-1,2-diol from (293.15 to 328.15) K, *J. Chem. Eng. Data*. **53(1)**: 271–274(2008).

[40] Hemmat M., Moosavi M., Rostami A.A., Study on Volumetric and Viscometric Properties of 1,4-Dioxane and 1,2-Ethanediol/1,3-Propanediol Binary Liquid Mixtures, Measurement and Prediction, *J. Mol. Liq.*, **225(1)**: 107-117(2017).

[41] Zemánková K., Troncoso J., Romaní L., Excess Volumes and Excess Heat Capacities for Alkanediol+Water Systems in the Temperature Interval (283.15–313.15)K, *Fluid Phase Equilib*. **356(1)**: 1–10 (2013).

[42] Zorębski E., Lubowiecka-Kostka B., Thermodynamic and Transport Properties of (1,2-Ethanediol+1-Nonanol) at Temperatures from (298.15 to 313.15)K, *J. Chem. Thermodyn*. **41(1)**: 197–204 (2009).

[43] Tsierkezos N.G., Molinou I.E., Thermodynamic Properties of Water + Ethylene Glycol at 283.15, 293.15, 303.15, and 313.15 K, *J. Chem. Eng. Data*, **43(1)**: 989–993(1998).

[44] Naidu B.V.K., Rao K.C., Subha M.C.S., Densities and Viscosities of Mixtures of Some Glycols and Poly Glycols in Dimethyl Sulfoxide at 308.15 K, *J. Chem. Eng. Data.* **47(1)**: 379–382(2002).

[45] George J., Sastry N.V., Densities, Dynamic Viscosities, Speeds of Sound, and Relative Permittivities for Water + Alkanediols (Propane-1,2-and -1,3-Diol and Butane-1,2-, -1,3-, -1,4-, and -2,3-Diol) at Different Temperatures, *J. Chem. Eng. Data*, **48 (1)**: 1529-1539(2003).

[46] Azarang N., Movagharnejad K., Pirdashti M., Ketabi M., Densities, Viscosities, Refractive Indices and Excess Properties of Poly (Ethylene Glycol) 300+1,2-Ethanediol, 1,2-PPropanediol, 1,3-Propanediol, 1,3-Butanediol and 1,4-Butanediol Binary Liquid Mixtures, *J. Chem. Eng. Data*, **66(7)**: 3448-3462 (2020).

[47] Riddick J.A., Bunger W.B., Sakano T.K., "Organic Solvents: Physical Properties and Methods of Purification", 4th Edition, Wiley-Interscience, New York (1986).

[48] E Zorebski., M Dzida., Piotrowska M., Study of the Acoustic and Thermodynamic Properties of 1,2-and 1,3-Propanediol by Means of High-Pressure Speed of Sound Measurements at Temperatures from (293 to 318) K and Pressures up to 101 MPa, *J. Chem. Eng. Data*, **53(1)**: 136–144(2008).

[49] Hawrylak B., Gracie K., Palepu R., Thermodynamic Properties of Binary Mixtures of Butanediols with Water, *J. Sol. Chem.*, **27(1)**: 17-30(1998).

[50] Geyer H., Ulbig P., Görnert M.. Measurement of Densities and Excess Molar Volumes for (1, 2-Ethanediol, or 1, 2-Propanediol, or 1, 2-Butanediol+ Water) at the Temperatures (278.15, 288.15, 298.15, 308.15, and 318.15) K and for (2, 3-Butanediol+ Water) at the Temperatures (308.15, 313.15, and 318.15) K, *J. Chem. Thermodyn.*, **32(1)**: 1585-1596 (2000).

[51] Checoni R.F., Experimental Study of the Excess Molar Volume of Ternary Mixtures Containing {Water+(1, 2-Propanediol, or 1, 3-Propanediol, or 1, 2-Butanediol, or 1, 3-Butanediol, or 1, 4-Butanediol, or 2, 3-Butanediol)+ Electrolytes} at a Temperature of 298.15 K and Atmospheric Pressure, *J. Chem. Thermodyn.* **42(1)**: 612-620(2010).

[52] Rackett H.G, Equation of State for Saturated Liquids, *J. Chem. Eng. Data.* **15(1)**: 514-517(1970).

[53] Yamada T., Gunn R.D., Saturated Liquid Molar Volumes. Rackett Equation, *J. Chem. Eng. Data.* **18(1)**: 234-236(1973).

[54] Li C.C., Critical Temperature Estimation for Simple Mixtures, *Can J. Chem. Eng.*, **19(1)**: 709-710(1971).

[55] Chueh P.L., Prausnitz J.M., Vapor-Liquid Equilibria at High Pressures. Vapor-Phase Fugacity Coefficients in Nonpolar and Quantum-Gas Mixtures, *Ind. Eng. Chem.*, **6(1)**: 492-498(1967).

[56] Puig Arnavat M., Bruno J. C.,"Artificial Neural Networks for Thermochemical Conversion of Biomass". In Pandey A., Bhaskar T., Stöcker M., Sukumaran R. (Eds.), "Recent Advances in Thermo-Chemical Conversion of Biomass" (pp. 133–156). Elsevier. https://doi.org/10.1016/B978-0-444-63289-0.00005-3 (2015).

[57] K Passino.M., Biomimicry of Bacterial Foraging for Distributed Optimization and Control. Control Systems, *IEEE Control Syst..* **22(3)**: 52-67(2002).

[58] Sorensen K., Metaheuristics—the Metaphor Exposed, *Int. Trans. Oper. Res.*, **22(1)**: 3-18 (2015).

[59] Tovey C.A., "Nature-Inspired Heuristics: Overview and Critique. Recent Advances in Optimization and Modeling of Contemporary Problems", INFORMS. (2018).

[60] Lones M.A., Mitigating Metaphors: A Comprehensible Guide to Recent Nature-Inspired Algorithms, *SN Computer Science*, **49(1)**: 1-12 (2020).

[61] Niu B., Wanng J., Wang H., Bacterial-Inspired Algorithms for Solving Constrained Optimization Problems, *Neurocomputing*, **148(1)**: 54-62 (2015).

[62] Priddy K., Keller P., "Artificial Neural Networks: An Introduction", Washington, SPIE Press. (2005).